

## Chapter 01: Introduction

---

### 1.1 Metallic Glass

Generally cooling a molten liquid below its melting results in the formation of a crystalline structure. Crystalline structures belong to one of the 14 Bravais lattices and 32 crystallographic groups. However, if somehow crystallization is prevented, the molten liquid can solidify with a disordered atomic structure. Such materials are known as ‘metallic glasses. By definition, metallic glasses are substances that solidify without crystallization below the glass transition temperature ( $T_g$ ). The glass-transition temperature can be defined as a temperature below which the viscosity reaches  $10^{13}$  Pa. s and it is well below the melting temperature ( $T_m$ ). Historically, the first metallic glass was synthesized by Pol Duwez and his co-workers at the California Institute of Technology (Caltech) in Pasadena, California. They synthesized an Au-25 at. % Si alloy in the glassy state by rapidly solidifying the molten liquid at cooling rates between  $10^5$ - $10^6$  K/s[1]. Following this discovery, a very large number of alloy compositions were studied for the glassy state[2]–[4]. These metallic glasses were produced in the form of ribbons (<1mm thickness), wires, or powders ( $\sim\mu\text{m}$ ) only. This restriction on the section thickness has prohibited the widespread use of these glassy materials. For example, glassy alloys in ribbon or wire form in the Fe-Si-B and Co-Fe-Si-B systems have been used as soft magnetic materials[5]–[7], but there have not been any reports regarding applications of these novel materials in the field of as structural or as functional materials.

### 1.2 Bulk Metallic Glasses

Metallic glass composition that displays large section ( $\sim\text{mm}$ ) thickness. They have high glass-forming abilities. They are known as Bulk Metallic Glasses (BMGs)[4]. In the last 30 years, intensive development has been observed in BMGs having Co-[8], Fe-[9], Cu-[10], Zr-[11], Pd-[12], Ti-[13] based alloys. BMGs have been produced by many researchers with critical diameters exceeding 10mm[4]. Among all the BMG alloys, it was observed that Fe-based BMG alloys are very attractive due to their excellent magnetic properties, high electrical resistivity, high corrosion resistance, high mechanical properties as well as relatively low material cost[14], [15]. The first Fe-based BMG alloy was synthesized by Inoue and his co-workers[9] in the Fe-Al-Ga-P-C-B system in 1995 by applying a Cu-mould casting technique. Following this discovery, a very large number of Fe-based bulk-metallic glasses have been developed to date. Table 1.1 shows some typical Fe-based BMG reported by Suryanarayana and Inoue [4] with calendar year.

**Table 1. 1:** Fe-based BMG alloy system reported together with the calendar years[4]

Sl.no.	Alloy	Year of report of synthesis	Critical diameter(mm)	Remarks
1.	Fe- (Al, Ga)- (P, C, B)	1995	1	First synthesis
2.	Fe- (Cr, Mo)- (Al, Ga)- (P, C, B)	1996	-	Addition of ETM (Cr+Mo)
3.	Fe- (Co, Cr, Mo.)- (Ga, Sb)- (P, C, B)	1999	4	Largest in this series
4.	Fe-Ga- (P, C, B, Si)	2000	1	ETM+Al free
5.	Fe- (Zr, Hf, Nb, Ta)-B	1997	6	ETM
6.	Fe-Ln-B	1999	-	Addition of Ln
7.	Fe- (Cr, Mo)- (C, B)	2001	-	Cr+Mo (improve corrosion resistance)
8.	Fe- (B, Si)-Nb	2002	1	Nb From ETM
9.	Fe- (Si, B, P)	2008	2.5	ETM free
10.	Fe-Mn-Cr-Mo-C-B	2003	4	Mn, Mo, C
11.	Fe-Cr- (Ln, Y)-Mo-C-B	2004	12	Y and Ln
12.	Fe- (Co, Cr, Mo)- (C, B)-Y	2005	16	ETM + Y (largest in this series)
13.	Fe- (Cr, M o)- (C, B)-Y	2006	10	Tm (improve corrosion resistance)

### 1.3 Concept of Glass Formation

The concept of glass formation is related to the variation of specific volume with temperature. Generally, the volume of most of the crystalline materials decreases with a decrease in temperature from the liquid state. Figure 1.1 shows the variation of specific volume as a function of

temperature. After reaching the freezing temperature, there is a significant drop in the specific volume of the metal until it reaches a characteristic value of the crystalline state. A liquid normally undercools before crystallization begins. This is due to an activation energy barrier that needs to be overcome before solid nuclei form in the melt.

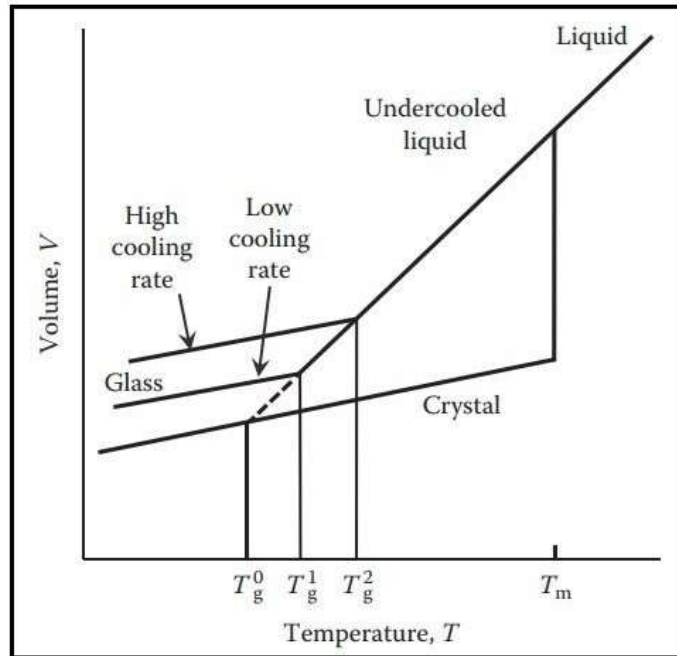


**Fig. 1. 1:** Variation of specific volume with temperature for metal and glass-forming metals[15].

But, in the case of glass-forming liquid, the liquid can be significantly undercooled either due to the imposition of a high cooling rate or the removal of heterogeneous nucleating sites. The volume even decreases in the undercooled region and its viscosity continues to increase. The viscosity reaches so high and the liquid gets frozen. This frozen liquid is referred to as glass[16].

It is essential to understand the fundamental reason behind the amorphous or glassy phase formation in metallic alloys. The glassy phase forms when the liquid alloys are supercooled significantly to a temperature below the glass transition ( $T_g$ ) temperature such that the formation of crystal nuclei is completely suppressed. When the liquid alloy is rapidly quenched (supercooled liquid) at a critical cooling rate ( $R_c$ ), beyond it will be frozen into a solid without crystallization. A temperature-time-transformation (TTT) diagram during liquid-solid phase transformation has been shown in Fig. 1.2. The  $R_c$  can be estimated from this.

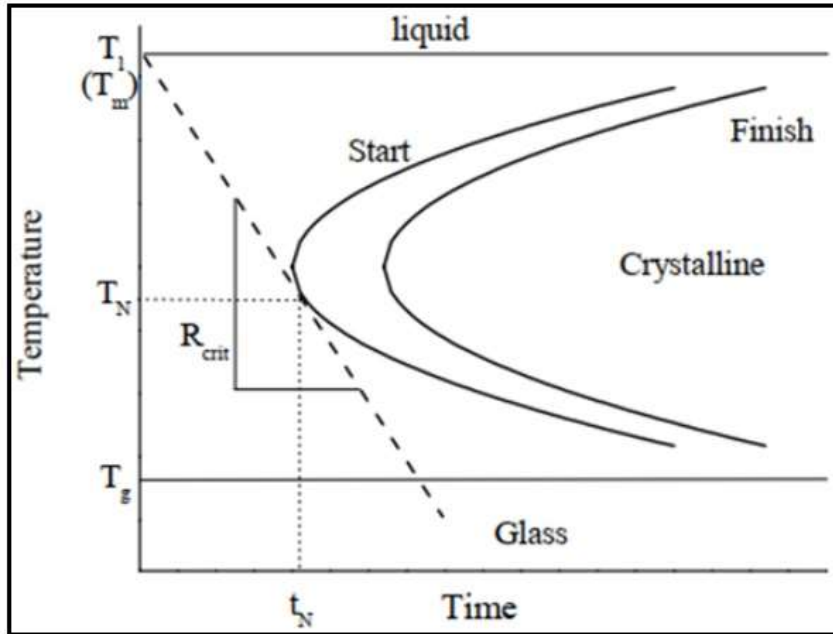


**Fig. 1. 2:** Schematic representation of T-T-T diagram during solid-liquid transformation[17]

T-T-T diagram. The diagram represents two C-shaped curves representing the start and completion of crystallisation events within a particular temperature range. Here critical cooling rate can be defined as the slope of the dashed line that touches the nose of the start C-curve of crystallisation. The critical cooling rate for glass formation can be written as:

$$R_c = (T_1 - T_N)/t_N$$

Where  $T_1$  is the liquidus temperature,  $T_N$  is the temperature at the nose of the T-T-T diagram and  $t_N$  is the time required for the nucleation of the first crystallite. If the critical cooling rate is low, it will be easier for glass formation. Therefore, for easy glass formation, the nose of the C-curve should shift towards the right side.

The points of the start of the C-curves in the three different materials, Pure metals, marginal glass, and bulk-metallic glass are shown in Fig. 1.3. In conventional crystalline alloys, the nose of the start of the crystallization curve is very near to the Y-axis so that the cooling rate required for these alloys as high as  $10^5$ – $10^6$  °C/s. For the metallic glasses, the C-curve shifted towards the right and  $R_c$  is of the order of  $10^5$ - $10^6$  °C/s, whereas in the case of bulk-metallic glasses, the position of the C-curve is far away from the Y-axis. As a result, a very slow cooling rate in the order of  $10$  - $10^2$  °C/s will be sufficient to obtain a glassy phase.

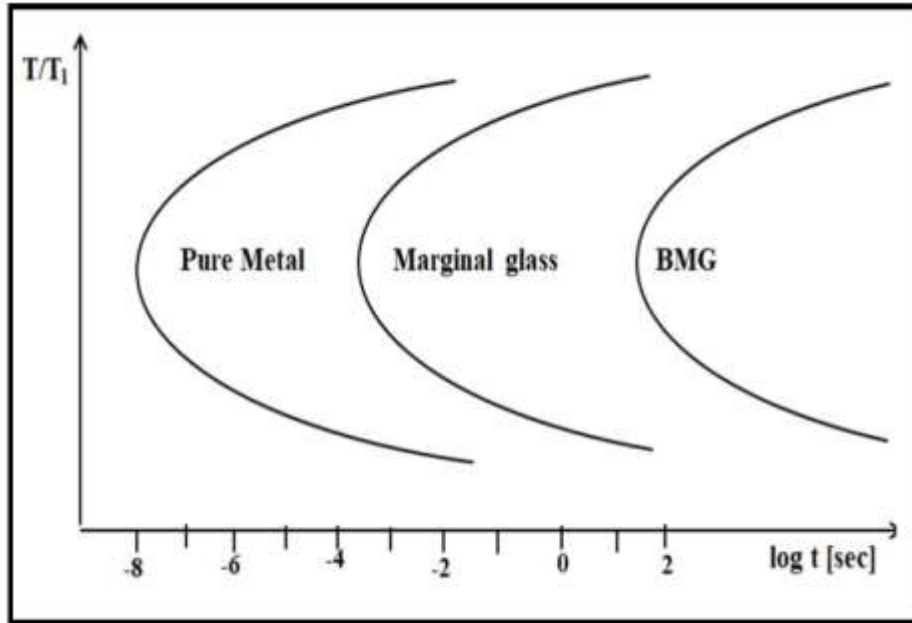


**Fig. 1. 3:** Schematic representation of T-T-T diagram for pure metals, metallic-glass and bulk-metallic glass[17]

#### 1.4 Glass Forming Ability (GFA) and Glass Forming Criteria

The ability of a metallic alloy to transform into a glassy state is termed as glass-forming ability (GFA)[4]. From the alloy design point of view, several criteria were proposed for the prediction of glass formation. Greer (1993)[18], proposed the famous theory, known as the “confusion principle”, which is based on the multi-component system. According to this theory, the GFA of BMGs increases with the increase in the number of constituent elements. The greater number of constituent elements will retard the formation of competing crystalline phases during cooling. Most of the Fe-based BMGs with a higher GFA are all multi-component alloys having 4 to 9 constituents. Inoue (2000)[19], proposed “three empirical rules” guiding the design of Fe-based BMGs. They refer to, (i) multi-component systems consisting of more than three elements, (ii) a significant difference in atomic size with size ratios above 12% among the main three constituent elements, and (iii) the enthalpy of mixing among the three main constituent elements should be negative. The alloys satisfying these empirical rules have special atomic clusters in the liquid state, which is beneficial to promoting glass formation [19]. The GFA of any system involves two aspects. They relate to (i) the stability of the liquid structure, and (ii) the resistance to crystallization. The former refers to the geometry of clusters and the latter pertains to the kinetic factors[20]. Bernal[21] advocated the glass-forming tendency of the metals based on the dense random packing (DRP) of the hard-sphere for a single-component system in the liquid state. Later

in a multi-component system, the combination of constituent elements having differences in radii as well as the negative heat of mixing[19] was seen to yield efficient packing of clusters(ECP)[22] and consequently increased the density of random packing of atoms in the super-cooled liquid state. Egami and Waseda[23] proposed the atomic volume strain criterion to predict GFA in binary alloys produced by the RSP technique. According to them, a minimum solute concentration is required to produce critical strain for destabilising the crystal lattice. The density difference between the structurally relaxed and fully glassy state is about 0.11-0.15%. Thus, the small density difference between them suggests that glassy alloys contain dense randomly packed clusters in them[24]. Bota et al. [25] developed a new criterion to predict GFA based on electronegativity difference. Small differences in electronegativity tend to the formation of solid solutions otherwise stoichiometric compounds will form. Some researchers[26]–[29] have proposed simple parameters and tried to correlate them with GFA. These parameters are the kinetics process, nucleation growth rate, and crystal growth rate[30]. Kinetically, high GFA is related to the viscosity of the liquid alloy[31]. When viscosity changes for temperature, known as fragility and it occurs around glass transition temperature ( $T_g$ )[32]. The concept of fragility was first proposed by Angell[32]. The fragility parameter ( $m$ ) is inversely correlated to critical thickness ( $D_c$ ) and directly correlated to the critical cooling rate ( $R_c$ )[33]. Azad et al.[34], have proposed a Venn diagram for evolving criteria for metallic glass formation in terms of three parameters. These are (i) electron-to-atom ratio ( $e/a$ ), (ii) volume ratio ( $V_R$ ), and (iii) radius ratio ( $R_R$ ). In addition to these, they have also invoked the Fermi wave vector ( $KF$ ) and Pseudo Brillouin zone ( $PBZ$ ) concepts for assessing their interactions in stabilizing the unique composition of the alloy. In addition to these principles, numerous GFA indicators such as  $T_{rg}$ ,  $\Delta T_x$ ,  $\gamma$ ,  $\alpha$ ,  $\beta$ ,  $\delta$ ,  $\phi$  and  $\omega$  have been also proposed for quick GFA evaluations[4], [19], [35].

In a critical assessment of the above-proposed criteria, it was noticed that no single criterion can provide a satisfactory explanation about the GFA of the BMGs, although they provide some useful direction in the development of BMGs. The GFA depends on many factors such as alloy composition, interaction among constituent elements, atomic size factor and even fabrication methods. Thus, it is really difficult to determine which criterion is more effective for the prediction of GFA of BMGs, especially for Fe-based BMGs. Generally, Fe-based BMGs have lower GFA. Therefore, the synthesis of Fe-based BMGs is mostly based on “trial and error” method [36].

## **1.5 Fabrication Techniques and their Influences on Glass Formation and Properties**

### **1.5.1 Preparation Methods for Fe-based BMGs**

Owing to limited GFA in Fe-based metallic glasses, amorphous ribbons were fabricated by using a single roller melt-spinning technique or splat quenching methods as there is a fast cooling rate of  $10^5$ - $10^6$  K/s[4], [15], [37], [38]. After that lots of novel multi-component Fe-based alloys were fabricated using injection-casting and suction-casting of the molten alloys into copper-mould[4], [15], [37]–[39]. These two methods significantly improved the GFA. In addition, the drop-casting technique also improved the GFA(critical thickness  $\sim 10$ mm) in Fe-based BMGs containing rare-earth[40], [41]. In recent years many more techniques were also developed for the fabrication of Fe-based BMGs, they are sequentially, centrifugal-casting[40]-[41], mechanical alloying[36], [44], [45], the compaction of powder by cold pressing, hot pressing or pulse current sintering[46]–[48], spark-plasma sintering[49]–[51] and pressure die-casting[52].

In 2003, a special device was invented by Gan et al.[53]. They designed a new Cu-mould casting setup as shown in Fig.1.4 by combining flux melting and Cu-mould casting methods. By the use of this new device, a large undercooling as well as fast cooling could be achieved. They prepared Fe-Ni-P-B-Ga system-based BMGs with a 3mm diameter[53]. Using a similar setup by Stoica et al.[54] in 2006 produced the first ternary Fe-Nb-B BMGs.

Another interesting method, known as the J-quenching technique was specially designed for the fabrication of Fe-based BMGs[55], as shown in Fig. 1.5. To fabricate BMGs by using the J-quenching method, the master alloy is loaded at the bottom of the upper tube. The J-shaped tube is connected to an evacuating pump, and high-purity argon gas is filled, once the system reaches a certain vacuum. The ingot is then melted and pushed into the smaller fused tube with the help of argon gas. Subsequently, the entire J system is transferred to a furnace which has a heating coil. The ingot placed in a smaller tube will be heated above the liquidus temperature and held there for some time so that the metal liquid can stabilize at that temperature. After that tube with the sample will be removed from the furnace and quenched in salted ice water.

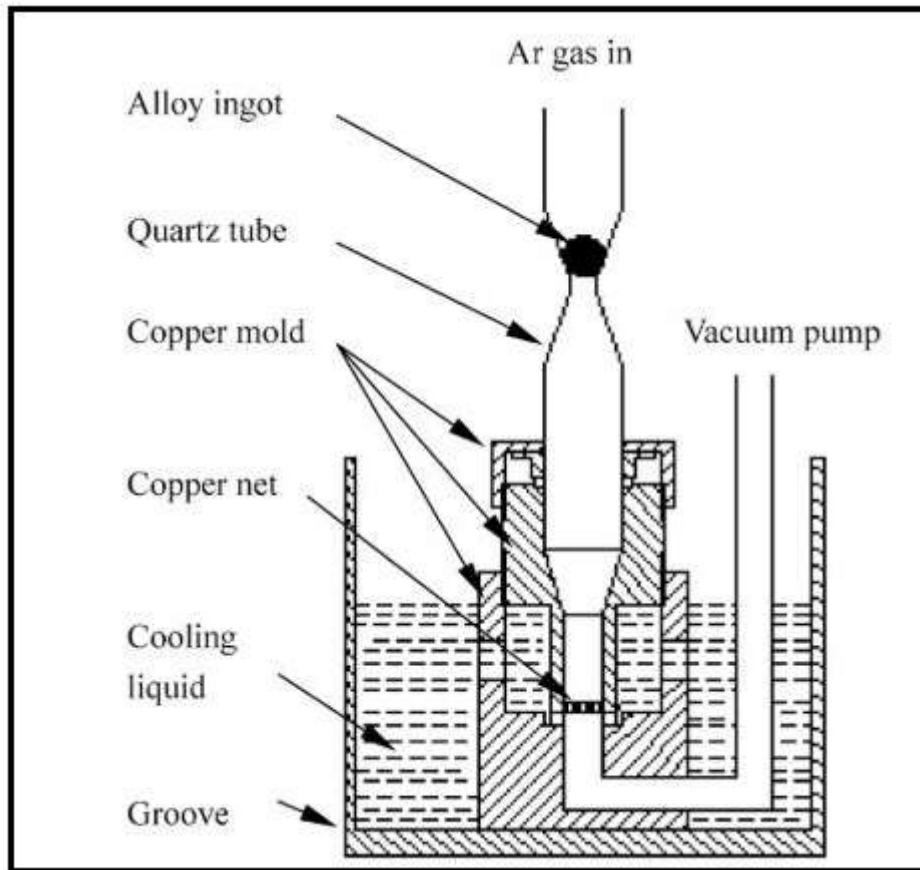


**Fig. 1. 4:** Schematic diagram of a new Cu-mould casting set-up invented by Gan et al.[53]

In the literature, most studies aim at preparing BMGs (up to maximum critical thickness ~10mm diameter) by using various casting techniques. In contrast, SPS has the most significant interest in the fabrication of novel BMGs/nanocrystalline materials[56]. The SPS process provides enormous possibilities for sintering highly dense nano-crystalline materials in a shorter processing time. In recent times, the combination of MA with SPS has shown enormous potential to produce BMGs. In addition, additive manufacturing or 3D printing technology has attractive attention in the field of fabrication of Fe-based BMGs or BMG composites[57]–[60]. In 2013, Pauly et al. [58] was produced Fe-Mo-P-C-B-Si based BMG by the selective laser melting technique. They formed amorphous powder and then melted by laser irradiation and built up layer by layer into a 3D BMG component but unfortunately, their samples were partially crystallized and induced cracks. It occurs due to large thermal stresses during the process. Despite this, Fe-based bulk sampling using the 3D printing technique is still a critical challenge because of the complexity and inherent drawbacks of this method.

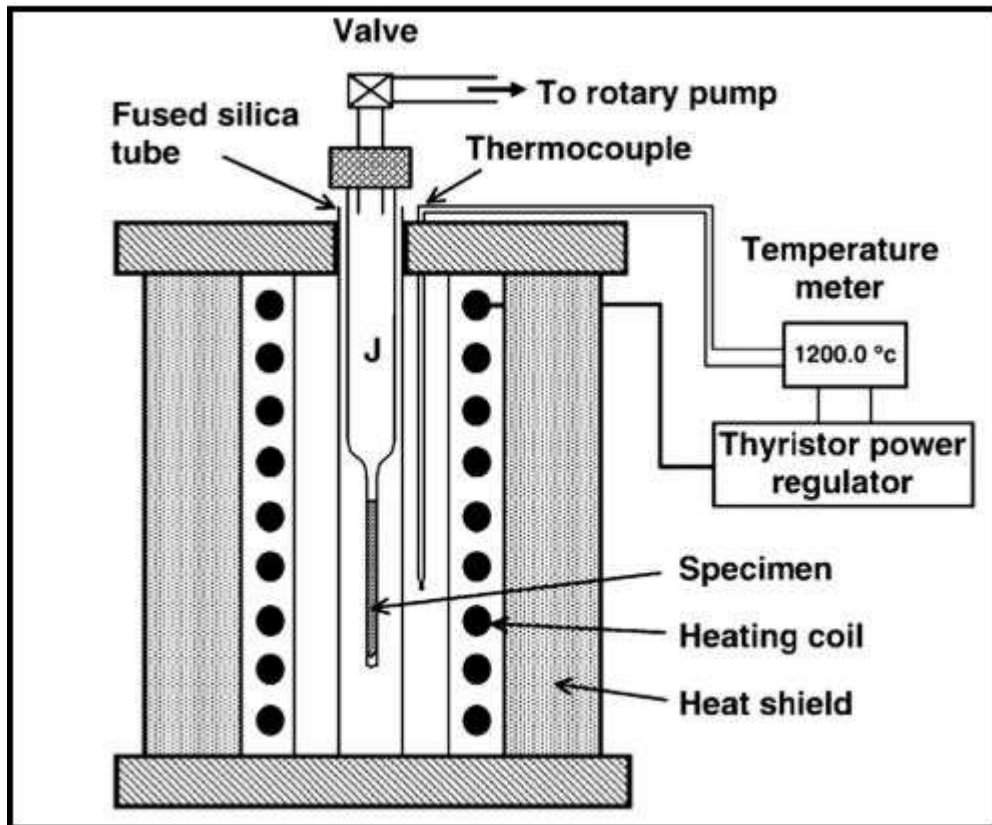


**Fig. 1. 5:** A Schematic diagram of the J-quenching set-up[55]

### 1.5.2 Effects of Cooling rate on glass formation and properties

The cooling rate plays a vital role in the formation of an amorphous structure. A fast-cooling rate applied to the liquid alloy kinetically facilitates the formation of an amorphous phase. The critical cooling rate ( $R_C$ ) which can be defined as the slowest cooling rate required to achieve a glassy structure, is sufficient to avoid crystallization in traditional casting process (e.g., Cu-mould casting method). Therefore, the  $R_C$  is a key criterion for evaluating the GFA of different alloys. For measuring the  $R_C$ , many methodologies have been developed including the theoretical approach proposed by Uhlmann[61], some experimental methods based on thermal analysis[62], [63], and wedge casting method[64], [65]. Lu et al.[66], reported that by use of helium as the fabrication atmosphere, instead of argon, the GFA can be improved. They produced a BMG rod of diameter 5mm in the argon atmosphere in the Fe-C-Si-B-P-Mo system and 7mm in the helium atmosphere. Helium can induce a faster cooling rate and it is considered the main reason for the improvement of GFA in this system. Helium can more easily suppress the precipitation of the competing crystalline phases as compared with that attained in the argon atmosphere. Masood and his co-workers[67] found that due to the reduction of the cooling rate microstructure also changes. In the Fe-B-Nb amorphous system, with the reduction of cooling rate, the samples transform from

amorphous structure to amorphous/nanocrystalline composites and then a fully crystalline structure.

It was observed that cooling rates also influence the soft magnetic properties of Fe-based BMGs. Gao et al.[66] found that in the Fe-C-B-Si-P-Mo BMGs system, the coercivity increased from 23.5 to 1.32 A/m when helium was used as a casting atmosphere instead of argon, but their saturated magnetization remained virtually unchanged.

In addition to the glass-formation and soft magnetic properties, the mechanical properties of the Fe-based BMGs are also influenced by the cooling rates[67]–[69]. For example Lesz[52], fabricated Fe-Co-B-Si-Nb based BMG rods with 2, 3, and 4mm diameter by pressure die-casting technique and measured the microhardness values at different distances from the outer edge of each rods. He found that near the edge the microhardness value is lower and it increases towards the centre of the rods. These results conclude that the faster the cooling rate during solidification lowered the microhardness. The SEM images of the Vickers' indentation impressions of Fe-Co-B-Si-Nb BMG rods with a 2mm diameter are shown in Fig. 1.6. In this figure three different positions (i.e. edge, middle, and central locations) of the BMG rod are observed. Fig1.6(a) depicts that multiple and semi-circular shear bands are formed around the periphery of the indentation impression, indicating good plastic deformation capability at the edge of the BMG rods. However, when moving towards the centre the shear bands disappear (fig.1.6(b)and(c)), indicating plasticity decreases. The variation of microhardness can be understood by the “free volume” concept in the edge, middle and centre parts of the rod.

In another study, Masood et al.[67] also noted that the same phenomenon was observed in Lesz's [70] results in the  $Fe_{71}B_{23}Nb_6$  BMG along the radial direction from the centre to the edge. They observed that the hardness and elastic modulus tend to decrease. They argued that this phenomenon is attributed to the ‘cooling rate that induced surface softening’.

### **1.5.3 Effects of oxide impurities on glass formation and properties**

The existence of various kinds of oxides becomes inevitable during the fabrication of Fe-based BMGs under industrial conditions. Therefore, it is of critical importance to investigate the effects of oxide on the GFA, mechanical, chemical and physical properties of Fe-based BMGs. Although such kinds of studies are limited in the literature. In 2009, Li et al.[71] reported regarding the role of oxides on GFA in Fe-based BMGs. They found that the critical size of fully amorphous rods

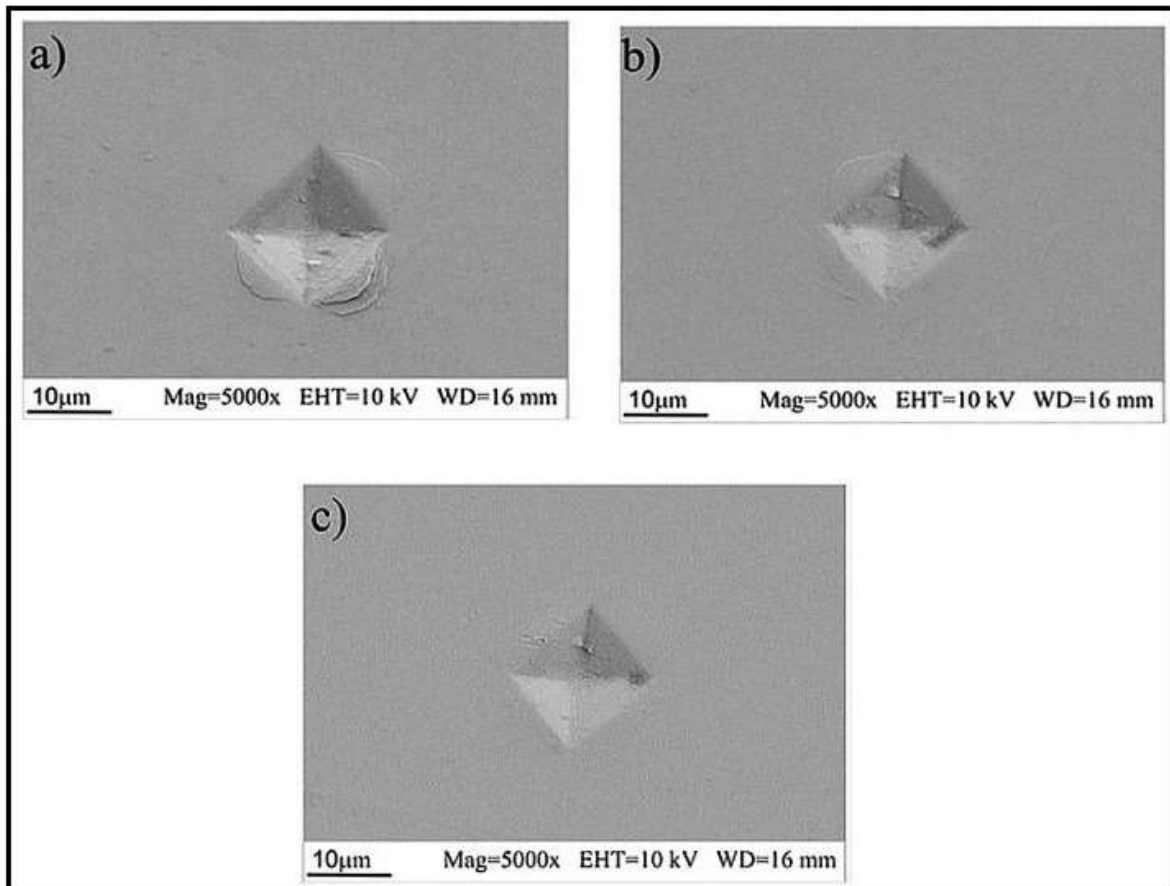


**Fig. 1. 6:** SEM images of indentation impression for different position, (a) edge, (b) middle, and (c) centre of  $\text{Fe}_{36}\text{Co}_{36}\text{B}_{19}\text{Si}_5\text{Nb}_4$  BMG rods with diameter of 2mm under loading of 200g[70].

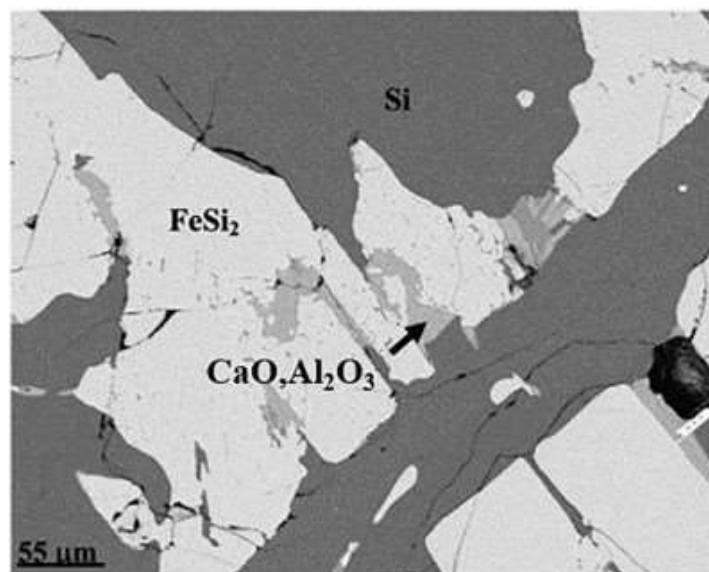


**Fig. 1. 7:** SEM back-scattered image of the industrial grade Fe-Si alloy[71].

it decreased from 5mm to 1mm if commercial Fe-Si pre-alloys were used instead of high purity of Si in  $\text{Fe}_{68.8}\text{C}_7\text{Si}_{13.5}\text{B}_5\text{P}_{9.6}\text{Cr}_{2.1}\text{Mo}_2\text{Al}_2$  BMG. The presence of CaO and  $\text{Al}_2\text{O}_3$  in the commercial Fe-Si alloys as shown in Fig. 1.7 are relatively strong catalysts, which can easily promote the crystallization of primary  $\alpha$ -ferrite phase and lower the GFA.

From a glass formation point of view the impacts of CaO and  $\text{Al}_2\text{O}_3$  on the GFA, it was recently reported that some rare-earth (RE) oxides behave as non-catalytic and can be used to purify the melt by scavenging the oxygen. It results in the GFA of Fe-based alloys that can be improved due to the minor addition of RE elements[40], [72]–[75]. Fig. 1.8(a-b) represents the backscattered electron microprobe micrographs of the central section of the 5mm drop-cast samples for the  $\text{Fe}_{63}\text{Zr}_8\text{Co}_6\text{Al}_1\text{Mo}_7\text{B}_{15}$  and  $\text{Fe}_{60}\text{Zr}_{7.8}\text{Co}_6\text{Al}_1\text{Mo}_{6.9}\text{B}_{16.6}\text{Y}_{1.8}$  alloys respectively. Fig. 1.8(a) shows the alloy without the addition of Y, having a dendritic structure embedded in the amorphous matrix, while with the minor addition of Y the GFA was improved so that 5mm amorphous rod containing some spherical dark particles (i.e. yttrium Oxides) as shown in fig. 1.8(b) was formed.

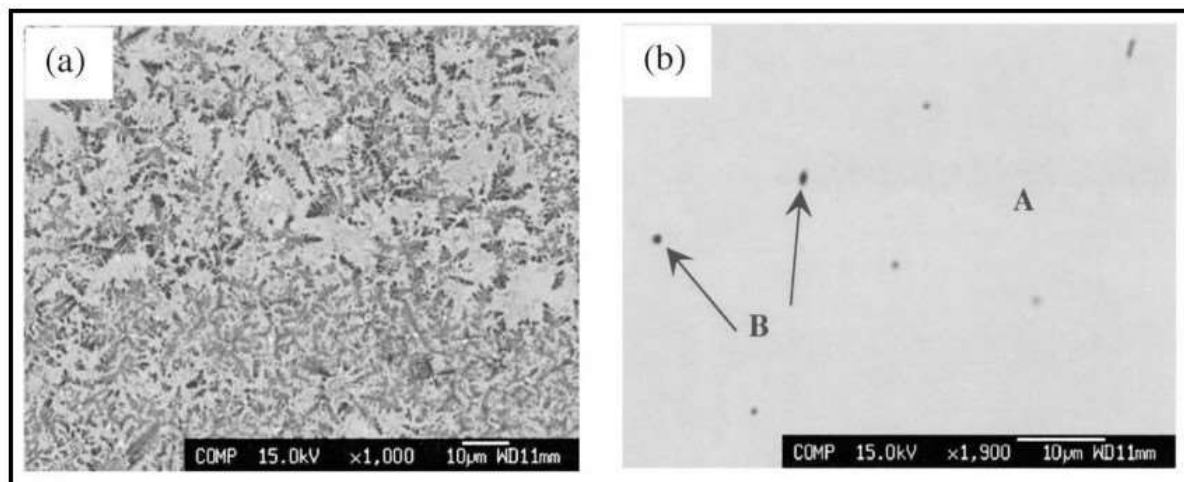


**Fig. 1. 8:** Backscattered electron microprobe micrographs for the central part of 5mm drop-cast samples for the alloys (a)  $\text{Fe}_{63}\text{Zr}_8\text{Co}_6\text{Al}_1\text{Mo}_7\text{B}_{15}$  and (b)  $\text{Fe}_{60}\text{Zr}_{7.8}\text{Co}_6\text{Al}_1\text{Mo}_{6.9}\text{B}_{16.6}\text{Y}_{1.8}$  [76]

In addition, the oxides can also influence other properties of Fe-based BMGs. It was reported by many researchers[77]–[79], the oxides can influence the structural homogeneity and pitting occurs at the regions where oxide particles were formed. Thus, the overall corrosion resistance can be decreased due presence of these oxides. Liu et al., [80] reported that due to the presence of oxides, the coercivity of the as-milled Fe-Ni-Zr-B-based alloy powders can be increased.

## 1.6 Crystallization behaviour

Metallic glasses, whether produced by a melt-spinning process in the form of ribbons at high solidification rates or in bulk form by conventional solidification methods relatively at slower solidification rates, are always in a high-energy or metastable state. Consequently, they release their energy by transforming into the crystalline state, which is referred to as crystallization or devitrification[81].

When a metallic glass sample is heated at a constant heating rate, typically between 5-20 K/s, the transformations take place in the sample. They are indicated peaks in the differential scanning calorimeter (DSC) or a differential thermal analyser (DTA) curve. Due to continuous heating, the glassy alloy shows a glass transition temperature ( $T_g$ ), one or more crystallization temperatures ( $T_x$ ), and an endothermic peak corresponding to melting ( $T_m$ ) of the alloy. Crystallization of a metallic glass taking place at or above  $T_x$ . However, it is not a thermodynamic parameter like  $T_m$ , it is a function of the heating rate.

From both scientific and technological points of view, the crystallization studies of metallic glasses are important. Since the crystallization process of MGs arises due to the nucleation and growth process, it allows studying the growth of crystals into an isotropic medium. It has been noted that the crystallization temperature of metallic glasses provides a real upper limit of the safe use of MGs without losing their interesting combination properties[81].

Crystallization in MGs occurs by nucleation and growth process. The main driving force for this is the difference in the free energy between the glassy phase and the corresponding crystalline phases. The crystallization behavior of metallic glasses can be understood by hypothetical free energy versus composition diagram[82]. There are mainly three modes of transformation that are possible. They refer to (i) polymorphous crystallization, (ii) Eutectic crystallization, and (iii) primary crystallization.

### 1.6.1 Polymorphous Crystallization

In this mode of transformation, the glassy phase transforms into a single crystalline phase without any change in composition. The polymorphous crystallization occurs in a composition range where a glassy phase had formed at a composition corresponding to either a stable or metastable solid solution or an intermetallic phase. From Fig. 1.9, polymorphous crystallization is possible when a glassy phase is transformed into the  $\alpha$ -Fe solid solution (i.e. reaction 1) or the  $Fe_3B$  phase (i.e. reaction 4) or the  $Fe_2B$  phase. Since  $Fe_3B$  is a metastable

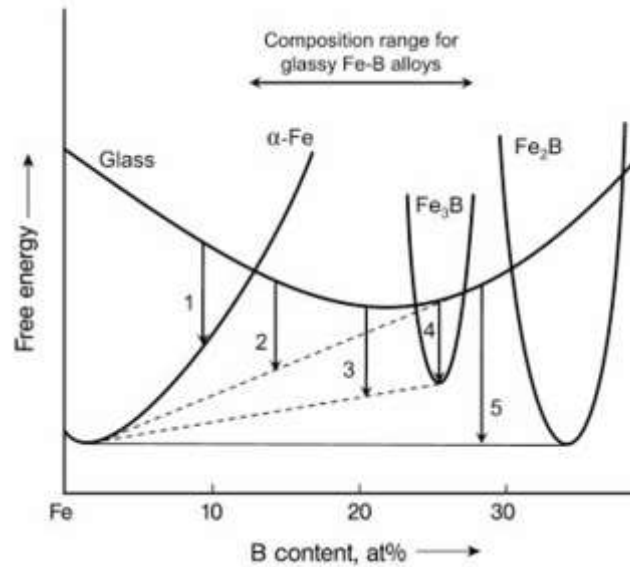


**Fig. 1. 9:** Hypothetical free energy vs. composition diagram for the Fe-rich, Fe-B alloy system[81].

phase, it will consequently transform into the equilibrium  $\alpha$ -Fe and  $\text{Fe}_2\text{B}$  phases on further annealing. Similarly, the supersaturated  $\alpha$ -Fe will also transform to the equilibrium constitution on further annealing. In polymorphous crystallization, the growth of the crystal is linear with time and the growth rate has an Arrhenius dependence on temperature. Such, a type of transformation mode is least common among the glass-crystal transformations. Fig. 1.10 (a) shows a bright field TEM micrograph of polymorphous crystallization in a  $\text{Ti}_{50}\text{Ni}_{25}\text{Cu}_{25}$  BMG alloy.

### 1.6.2 Eutectic Crystallization

In this mode of crystallization, the glassy phase transforms into two or more two crystalline phases by a discontinuous reaction. For example, in fig. 1.9, through reaction 3 the glassy phase can form a mixture of  $\alpha$ -Fe and  $\text{Fe}_3\text{B}$  or through reaction 5 it can form a mixture of  $\alpha$ -Fe and  $\text{Fe}_2\text{B}$  phases. This type of mode of crystallization has the largest driving force and can occur in the whole concentration range in between the two stable or metastable phases.

Eutectic crystallization is a discontinuous reaction like polymorphous crystallization. The overall composition of the crystal and glass are the same. Here, the growth rate of the crystal is independent of time until a very hard impingement with another crystal occurs. Fig. 1.10 (b) shows a TEM bright field image, showing eutectic crystallization in a  $\text{Zr}_{62.5}\text{Cu}_{22.5}\text{Al}_{10}\text{Fe}_5$  BMG alloy when annealed for 10 min at 713K.

### 1.6.3 Primary Crystallization

In primary crystallization mode, a supersaturated solid solution is formed. For example,  $\alpha$ -Fe, forms initially from the glassy phase (i.e. reaction 2) as shown in fig.1.9. Although, the concentration of the solute in the  $\alpha$ -Fe phase is less as compared to the glassy phase, the solute (i.e. boron) atoms are rejected into the glassy phase and the remaining glassy phase becomes enriched in boron until further crystallization is stopped. At this stage, a metastable equilibrium is established between  $\alpha$ -Fe and the glassy Fe-B phase with the new composition.

In metallic glasses, it is generally noticed that primary crystallization is the main mode of transformation. The resultant crystalline phase formed could be either a terminal solid solution or an intermediate phase. The morphology of the primary crystals is dependent on composition and their range from spherical to dendritic. Fig. 1.10 (c) shows a bright field TEM image obtained from  $\text{Ti}_{50}\text{Ni}_{20}\text{Cu}_{23}\text{Sn}_7$  BMG alloy on heating in a DSC at a heating rate of 40 K/min up to 787 K temperature. It could be noted that the fine crystallites are dispersed in a glassy matrix.

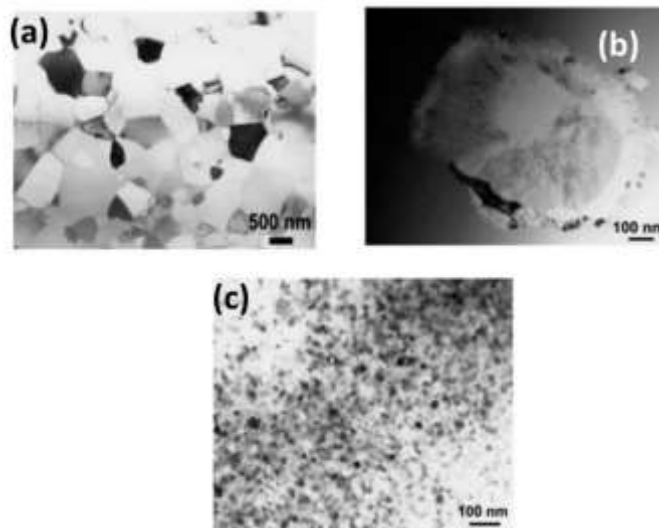


**Fig. 1. 10:** TEM images showing the microstructures obtained after (a) polymorphous crystallization, (b) eutectic crystallization, and (c) primary crystallization[81].

## 1.7 Mechanical behaviour of MGs/BMGs

### 1.7.1 Plastic deformation

In the absence of crystalline imperfections such as dislocations, grain boundaries and stacking faults, the mechanical properties of metallic glass are completely different from those of crystalline materials. The indentation technique is a significant tool for determining the mechanical properties of thin ribbons of MGs[83]. In the new generation of metallic glasses unlike

thin ribbons (i.e., BMGs) are fabricated by several new foundry techniques[19][84]. In literature, quite a few reports are devoted to examining the underlying deformation mechanism of BMGs using indentation techniques to explain their structural applications[85][86][87]. The plastic deformation behaviour of MGs/BMGs can be categorized into two different regimes, homogeneous and heterogeneous deformation, based on the materials' response to temperature and strain rate. At high temperatures (greater than  $\sim 0.5T_g$ ) low stresses and high strain rates, metallic glasses undergo viscous flow, where the plastic strains are continuously distributed within the material but not necessarily uniformly. This type of deformation is referred to as homogeneous deformation. Whereas, plastic flow at lower temperatures (below  $T_g$ ) and high stress and strain rates is referred to as heterogeneous deformation.

The nature of the inhomogeneous or heterogeneous deformation regime confines the usage of BMGs in engineering applications[88]. This kind of deformation is characterized by the formation of shear bands, their rapid propagation, and sudden fracture of the sample. Due to shear band formation, when these materials are loaded in tension, they exhibit negligible ductility before fracture. Leamy et al. [89] have reported that shear bands in MGs formed approximately on the planes of maximum resolved shear stress. These planes are inclined  $\sim 45^\circ$  to the tensile axis. Unlike crystalline materials, MGs have been shown to exhibit strain-softening behavior. That implies an increase in strain leads to softer material and allows the material to be deformed at lower stresses and higher rates. Shear band formation or shear localization is the main reason for strain softening in MGs. Since, MGs do not possess any microscopic heterogeneity (grain boundary, inclusions, or precipitates), the shear bands propagate without any obstacles and lead to catastrophic failure. Su et al.[90] reported that Zr-based BMGs fail catastrophically without any evidence of shear band formation. Therefore, the point can be noted that the formation of shear bands is the only signature of the presence of plasticity in metallic glasses not a reason for failure. Shear band formation or shear softening in MGs is attributed to a decrease in viscosity. Several reasons are available behind this. Some of the reasons are the production of free volume due to flow dilatation, redistribution of internal stresses related to shear transformation zone (STZ) operation, evaluation of structural order due to STZ operation, and local heating. All the reasons for inhomogeneous deformation due to the formation of shear bands are grouped under two hypotheses. The first hypotheses suggest that the viscosity in shear bands decreases during deformation. It is due to the formation of free volume in the MGs. This results in a decrease in the density of MGs and consequently its resistance to deformation. The second hypothesis suggests that the adiabatic heating occurs in the shear bands, which leads to a decrease in the viscosity of the MG by several orders of

magnitudes[89]. Some experimental evidence is available for both the increase in free volume and the rise in temperature in shear bands during deformation. Schuh et al.[91] studied the mechanism of a local increase in free volume as well as the evolution of structural order in metallic glass-derivative materials, in-situ and ex-situ composites, and nano-crystalline glasses. Schuch and Nieh[92] have surveyed the indentation tests on BMGs and reported the hardness as well as the onset of plasticity, the role of shear banding, and structural changes beneath the indenter.

### 1.7.2 The free volume model

Understanding the physical basis of the homogeneous deformation of BMGs is important. In practice, a homogeneous mode of deformation is of interest, particularly for shaping operations on MGs at high temperatures. The most widely used model which describes the homogeneous mode of deformation is the free-volume model. It was first proposed by Cohen and Turnbull[93] for liquids and applied to the glass-transition phenomenon and later it was adapted for the case of the deformation of MGs by Spaepen[94]. He arrived at the following flow equation:

$$\dot{\gamma} = 2\nu \exp(-\gamma v^*/v_f) \exp(-\Delta G^m/kT) \sinh(\tau\Omega/kT)$$

Where  $\dot{\gamma}$  is the viscoplastic strain rate,  $\nu$  is the atomic vibration frequency,  $\gamma$  is the shear strain,  $v^*$  is the atomic volume,  $\tau$  is the shear stress,  $v_f$  is the average free volume per atom,  $\Delta G^m$  is the activation energy of motion,  $\Omega$  is the atomic volume. This model states that deformation is a series of discrete atomic jumps in the MG, as shown in Fig. 1.11. (a), at sites where the excess free volume is high, and it is a diffusion-like process.

An experimental method to measure free volume and its changes on consequent thermal behavior performed by a differential calorimetric scan (DSC). The DSC experiment allows us to find glass transition for a glassy material. The exothermic hump just before the glass transition represents the energetics change between equilibrium and the metastable glassy state[95]. The ideal gas concept may be more suitable to understand this. In the equilibrium state of a glassy material, the atomic structure is believed to be packed or kinetically unable to permit atomic transport. Since atomic mobility is facilitated by the free volume. Those systems having higher free volume, indicate that the system is out of equilibrium state. Therefore, in a DSC thermogram, a bigger exothermic hump indicates a higher free volume available in the system. The work of Chen et al.[96] shows that a higher free volume content enhances the shear banding ability as well as yield strength of MGs depending on the amount of free volume content. As a consequence, the higher the free can also enhance the plasticity and toughness of BMGs[97], [98].

### 1.7.3 The Shear transformation zone (STZ) model

A smaller amount of free volume is required for the movement of atoms in the local shear transformation zone as compared to the diffusion process[99][100]. Therefore, a second kind of deformation unit developed by Argon in 1979[101] and confirmed by simulation studies, is referred to as STZ[102]. The STZ is a local cluster of atoms that undergoes an inelastic shear distortion from a low energy configuration to a next lower energy configuration by crossing of barrier of higher energy and volume. In contrast to the free volume model, the STZ includes a refined redistribution of several atoms over a diffused volume as shown in Fig. 1.11(b).

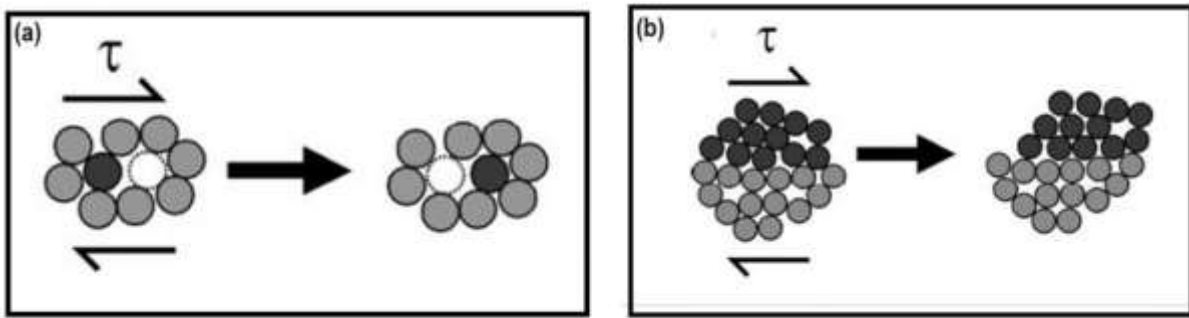


**Fig. 1.11:** Schematics representation of 2-D atomistic deformation mechanisms proposed for amorphous metals (a) the free volume model where diffusion-like atomic jumps showing accommodation of strain[94] and (b) the shear transformation zone model where the entire cluster shears over the other to achieve a new configuration[101].

Argon[101], reported two mechanisms for cluster motion at two different temperature regimes. According to him, a diffuse shear transformation occurs at a high temperature ( $0.6T_g > T > T_g$ ), and a concentrated shear transformation occurs at a low temperature ( $T < 0.6T_g$ ). The free energy barrier for the above transformation is given by[103][101]:

$$\Delta F_{STZ} = \left[ \frac{7-5\nu}{30(1-\nu)} G(T) \gamma_0^2 \Omega - \left( \frac{2(1+\nu)}{9(1-\nu)} G(T) \epsilon_v^2 \Omega - \frac{1}{2} \tau \gamma_0^2 \Omega \right) \right]$$

Where  $\nu$  is the Poisson's ratio,  $G(T)$  is the shear modulus (temperature dependent),  $\gamma_0$  and  $\epsilon$  are the shear and dilatational strain respectively,  $\tau_0$  is the interatomic shear resistance and  $\Omega$  is the STZ volume. It is assumed that the influence of free volume as STZs are activated where a region content higher free volume. Homer and Schuh[104] developed a finite element mesoscale approach that includes free volume as a state variable.

#### 1.7.4 Shear bands in metallic glasses

Shear band formation results in the accommodation or concentration of strain within a narrow zone. It is one of the outcomes of a material that can delocalize the strain and can affect an overall shape change. In crystalline solids, the formation of shear bands has been attributed to local heating during the dynamic loading. Polk and Turnbull[105] suggested that the formation of shear bands in BMGs is a result of structural disorder in the form of increased free volume and geometrical change in the cluster as well as compositional fluctuation.

#### 1.7.5 Bulk metallic glass composites (BMGs composites)

The major drawback with most BMGs is the lack of ductility and low fracture toughness except those who have high Poisson's ratio. The problem of brittleness in BMGs is generated by the hindrance of movement of shear bands, in such a way the shear bands either get blocked or deflected or even multiply as shown in Fig. 1.12. As a result, the number of shear bands increases which helps in homogeneous plastic deformation. BMG composites show much better mechanical properties, especially fracture toughness and plasticity the monolithic materials. Because of their special attribute, there have been several works in recent years on synthesizing and characterizing BMG composites growing rapidly[106]–[108]. The second phase can be added extrinsically or intrinsically.

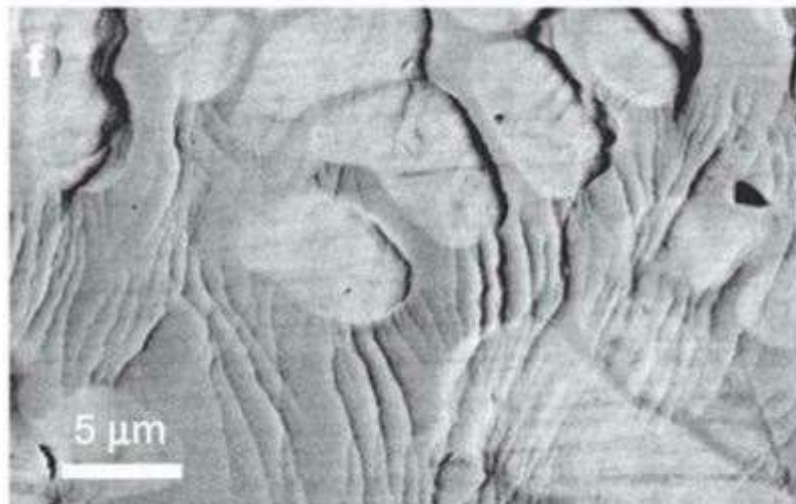


**Fig. 1. 12:** High magnification of a Zr-based BMG composite loaded in tension. The second phase promotes nucleation, multiplication, and arrest of shear bands[109].

### 1.7.5.1 In-situ BMG Composites

In situ composites are generally produced by either adjusting the alloy composition in such a way one phase will be crystallized and the other will solidify to obtain an amorphous phase, or secondary treatment after the complete amorphization such as annealing, hot extrusion of amorphous powders, etc. Fig.1.3 shows different types of precipitates formed, such as crystalline or quasi-crystalline phase, nano-crystallites, and dendrites, based on the cooling rate, temperature, and time required for the heat treatment.

Lu et al.[110] developed a series of metalloid-free Fe-based BMG matrix composites with a diameter of more than 10mm in Fe-Co-La-Ce-Al-Cu alloy. They noted that the melt phase-separated into Fe-rich and Fe-depleted liquids with further cooling, the Fe-rich liquid produced a mixture of body centered cubic-Fe (Co, Al) solid solution and Ce (Fe, Co)<sub>2</sub> intermetallic phase and remaining transformed into a glass. The final microstructure of the composite is shown in Fig. 1.14.

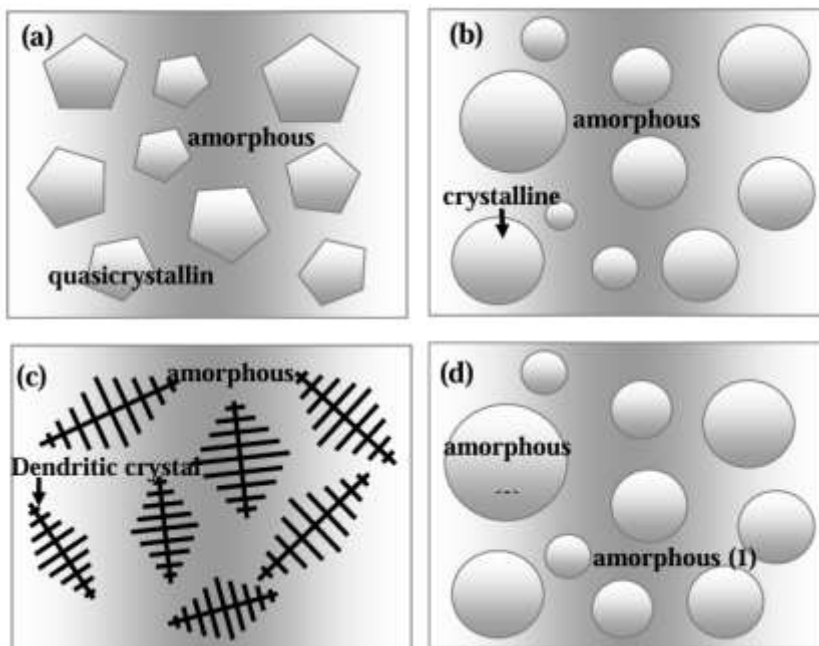


**Fig. 1. 13:** Different possibilities in in-situ composites (a) quasi-crystalline phase, (b) crystalline phase, (c) dendritic-crystalline phase, and (d) two different amorphous phases[109].

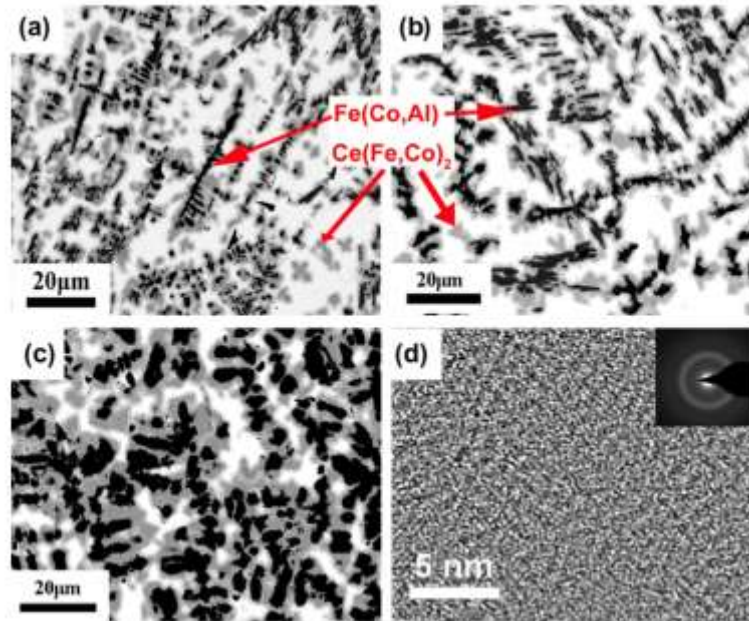


**Fig. 1. 14:** SEM micrographs for alloy (a) $Fe_{30}Co_{21}$  (b)  $Fe_{40}Co_{18}$  and (c) $Fe_{50}Co_{17}$  (d) HRTEM image and corresponding SAED patterns for the amorphous matrix in the  $Fe_{40}Co_{18}$  alloy[110].

Dong et al.[111] produced Fe-based composite by spark plasma sintering process with different sintering temperatures. The final product exhibits the highest microhardness (1168  $H_v$ ) and excellent wear resistance.

Zeng et al.[112] produced a Fe-based BMG composite by adding 40 vol.% Cu by using a selective laser melting (SLM) process in the FeCrMoCB system. Fig.1.15 shows a composite microstructure with the uniformly distributed crystal phase of Cu and amorphous Fe-based BMG and a well-bonding interface with a unique transition ring, which is beneficial to improve the mechanical properties of the Fe-based BMG composite.

Li et al.[113] produced BMG matrix composite of  $Fe_{77}Mo_5P_9C_{7.5}B_{1.5}$  alloy reinforced by in situ ductile  $\alpha$ -Fe dendrites has been formed. It shows a plastic strain of more than 30% and a high fracture strength of 3GPa.

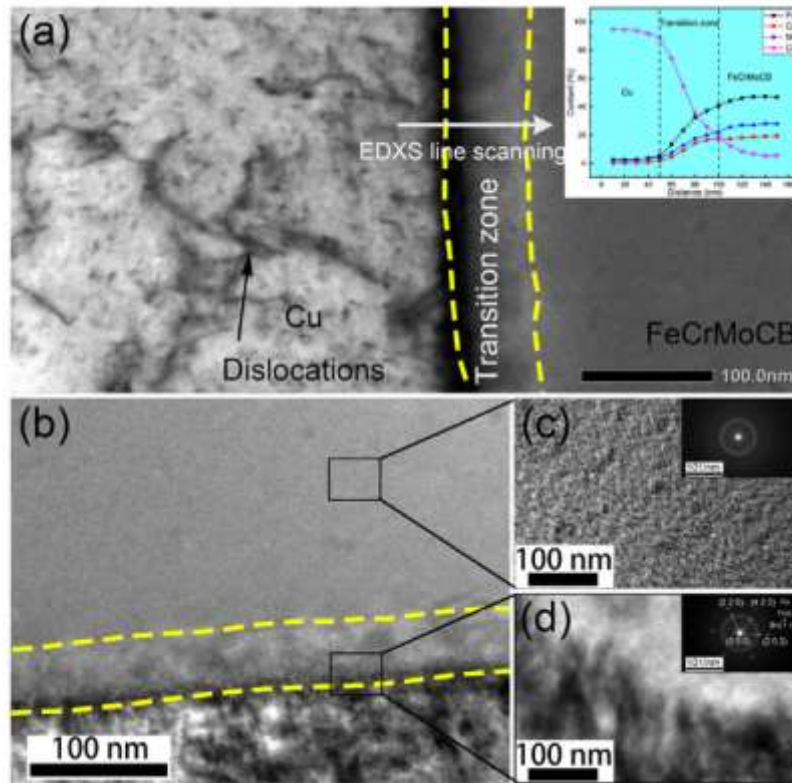


**Fig. 1. 15:** TEM images of SLM-fabricated Fe-based BMGCs with 40 vol.% Cu content: (a) Bright-field TEM image, (b) (c) (d) HRTEM images and corresponding SAED patterns of the interface.

### 1.7.5.2 Ex-situ BMG composites

This type of composite is prepared by introducing a second phase externally into the BMG matrix. The type of reinforcements used ductile metal fibers like Mo, W, Ta, Cu, and particles such as SiC, WC, W, Ta, and Mo have been added to the matrix, and a 900% increase in the compression strain to failure[114], [115]. The good wetting behavior of the glass-forming liquid with the reinforcement decides the strength and consistency of the interface. Although, it increases the chemical reaction between the reinforcement and the liquid melt. The strength and ductility of these composites depend on the volume fraction, size, morphology, and mechanical properties of the second phase. Therefore, the fabrication of these BMG composites needs a higher working temperature along with some protective coating on the interface to make it consistent. There are various methods are adopted to produce ex-situ BMG composites, inverted infiltration, infiltration casting, Cu-mould casting, liquid pressing, and powder metallurgy route[109].

## 1.8 Magnetic behaviour of MGs/BMGs

The magnetic properties of MGs/BMGs are of fundamental importance to several applications in the electrical and electronics industries. A large number of studies have been conducted by several researchers on Fe-based melt-spun ribbons. Duwez and Lin[116] have been started from the pioneering investigation of the Fe-C-P system in 1967. The most important application of melt-spun ribbons is in transformer core lamination based on their excellent soft magnetic behavior. A significant amount of effort has also been spent on investing in the magnetic properties of Fe-based BMGs. However, an important difference between the investigations on melt-spun ribbons and BMGs is that both metal-metalloid and metal-metal type alloys have been investigated in the thin film form, only metal-metalloid type alloys have been investigated in the BMG category.

It has been seen that the nature of magnetic behavior in BMG alloys has followed trends very similar to that of melt-spun ribbons. Several researchers have been studying the magnetic behavior of BMG alloy by using melt-spun ribbons. It was noted that there are minor differences in the melt-spun ribbons and BMGs, especially in those properties that are affected by structural relaxation, for example, magnetostriction and coercivity.

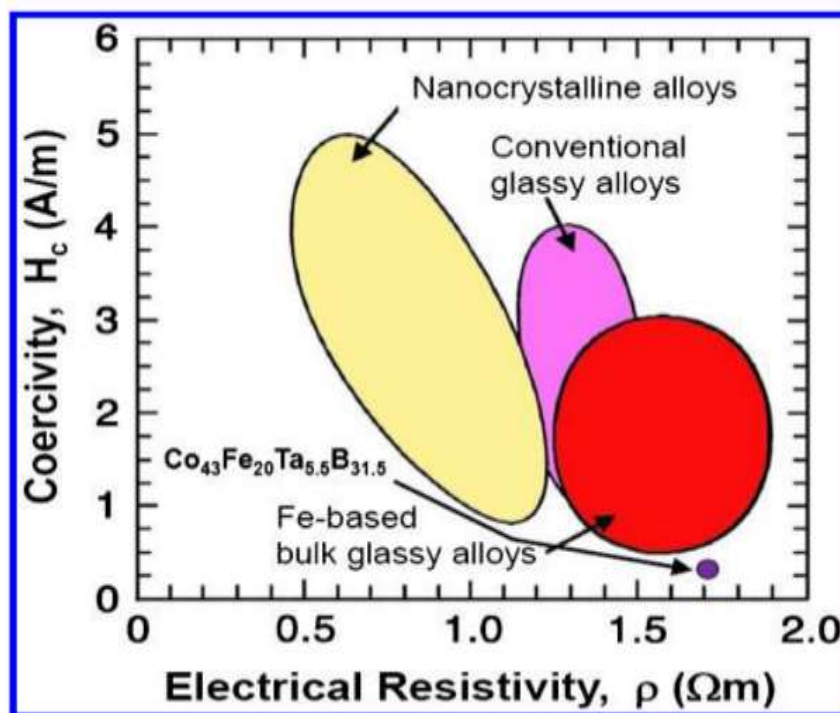


**Fig. 1. 16:** Relationship between coercivity and electrical resistivity for Fe- and Co-based glassy alloys[4].

The important features of the soft magnetic properties for Fe and Co-based glassy alloys in the Fe-TM-(P, C, B, Si) and (Fe, Co)-B-Si-Nb systems are summarised in Fig. 1.16.

In this figure, the relationship between coercivity and electrical resistivity for Fe- and Co-based glassy alloy has been shown. The data for conventional glass and nanocrystalline soft magnetic alloys are also included for comparison. It can be noted that Fe- and Co-based BMGs have a unique combination of very low resistivity and high electrical resistivity, such type of combination cannot be obtained in another kind of soft magnetic metallic material including glassy and nanocrystalline alloys.

### 1.9 Applications

Bulk metallic glass alloys display very high strength both in compression and tension, very high hardness, large elastic elongation limit, excellent corrosion resistance, and a good combination of soft magnetic properties. Recent progress in the development of BMG alloys like Zr-, Ti-, Co-, Fe-, Ni-, and Cu-based BMG alloys are used for magnetic sensing, chemical and structural applications. It was suggested[81] that the industrial applications of BMG alloys include: for magnetic applications such as linear actuators, magnetic cores, and choke coils; for chemical applications such as fuel-cell separators; and for structural applications such as sporting goods, precision gear for micromotors, precision optical parts, flowmeter, aircraft parts, automobile springs valve.

This thesis work is based on Fe-based glassy alloys. Therefore, based on current trends in the application of Fe-based BMGs this section focuses on only the application of Fe-based alloys like good soft magnetic properties and high strength for the use of soft magnetic and structural materials respectively. Some of the Fe-based alloys produced by several researchers and their applications are written in Table 1.2.

**Table 1.2: Some Fe-based alloys and their applications.**

Alloy	Existing nature	References details	Application
Fe <sub>61</sub> Cr <sub>4</sub> Mo <sub>14</sub> C <sub>15</sub> B <sub>6</sub>	Bulk	Ponnambalam et al., 2004[74]	Structural
	Ribbon	Duarte et al., 2014[117]	Electronic devices
	Powder	Ham et al., 2020[118]	Coating Coating

		Ahmed et al., 2022[119]	
$\text{Fe}_{48}\text{Cr}_{15}\text{Mo}_{14}\text{C}_{15}\text{B}_6\text{Y}_2$	Bulk	Iqbal et al., 2008[120]	Structural
	Bulk	Lu et al., 2014[121]	Structural & Functional
	Bulk	Liang et al., 2017[122]	Structural
$\text{Fe}_{45}\text{Cr}_{20}\text{Mo}_{10}\text{W}_2\text{C}_{15}\text{B}_6\text{Y}_2$	Bulk	Liang et al., 2017[122]	Structural
$\text{Fe}_{45}\text{Cr}_{15}\text{Mo}_{14}\text{Co}_3\text{C}_{15}\text{B}_6\text{Y}_2$	Bulk	Lu et al., 2004[40]	Structural & Functional
	Bulk	Chen et al., 2004[123]	Structural
	Bulk	Lu et al., 2014[121]	Structural & Functional

### 1.9.1 Soft magnetic materials

The outstanding soft magnetic properties of the Fe-based melt-spun ribbons are mostly used in power distribution transformers and many other applications. Due to their noncrystalline structure of MGs, the magnetic core loss is much less than in cold rolled grain-oriented silicon steels. However, these glassy ribbons not only reduce the eddy current loss but also less costly to produce thin ribbon tapes by cold rolling process for similar dimensions.

Soft magnetic glassy alloys belonging to the Fe-Tm-P-C-B-Si system have been commercialized by the trade name of Licalloy[38], [124]. The applications of the soft magnetic powder cores (i.e. ‘Licalloys cores’) in choke coils of AC-DC converters, DC-DC converters, noise suppression sheets, etc. The Licalloy powder core shows far better DC-superposed characteristics than those of Mn-Zn ferrite, also the same low core losses between Licalloy and Mn-Zn ferrite.

Furthermore, in comparison to Mn-Zn ferrite, the Licalloy powder inductor displays better DC-superposed characteristics in the elevated temperature range up to 393K. Through these advantages, the Licalloy powder core has been used as the power inductor in laptop-type computers because of their high efficiency and much smaller heat generation than those of any commercial power inductors, as shown in Fig. 1.17.

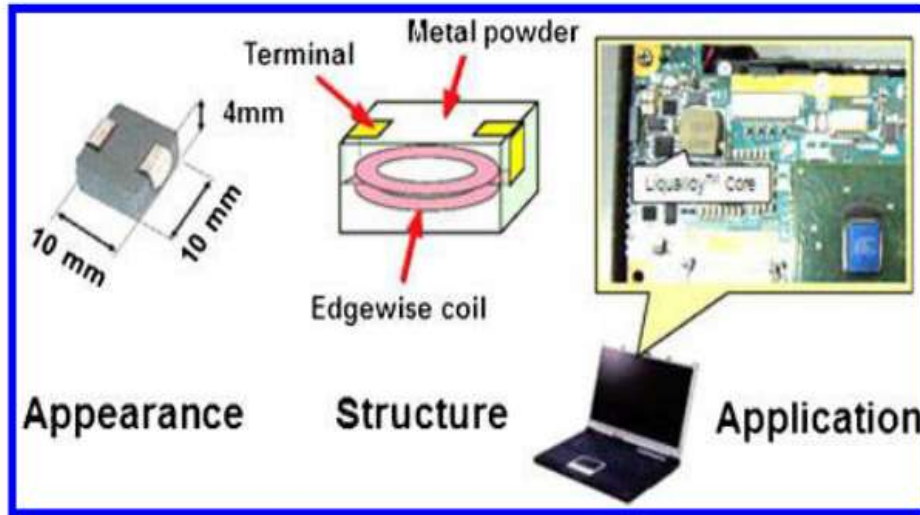


**Fig. 1. 17:** Licalloy powder core to power inductor in lap-top type personal computer[4].

The Licalloy powder produced by water atomization can be changed from a spherical shape to a flaky shape with a small thickness of 1-3  $\mu\text{m}$  by a bead milling operation. The resultant Licalloy sheet consisting of the flaky powder and resin and found to exhibit better electromagnetic noise suppression characteristics. Hence, Licalloy sheets have been used in digital still cameras.

### 1.9.2 Structural materials

The high yield or fracture strength, low Young's modulus, large elastic strain limit, and easy formability in the supercooled liquid region are the main characteristics of BMGs that make them attractive for structural applications. The large supercooled liquid region in BMGs provides an excellent opportunity to produce complex shapes easily. This is due to the plastic flow of the material in this temperature regime is Newtonian in nature. Through these advantages, BMG alloys have been extensively produced in different types of complex parts such as gears, coiled springs, and other complex parts. The parts using BMG alloy have complex shapes and sizes of these parts are much smaller than those that have been achieved by using conventional crystalline alloys.

Fe-based metallic glasses have very high yield strength and very high elastic limit as compared to crystalline steel and Ti alloys[35]. Fig. 1.18 represents the highest strength and Young's modulus of any BMG alloys than crystalline alloys.

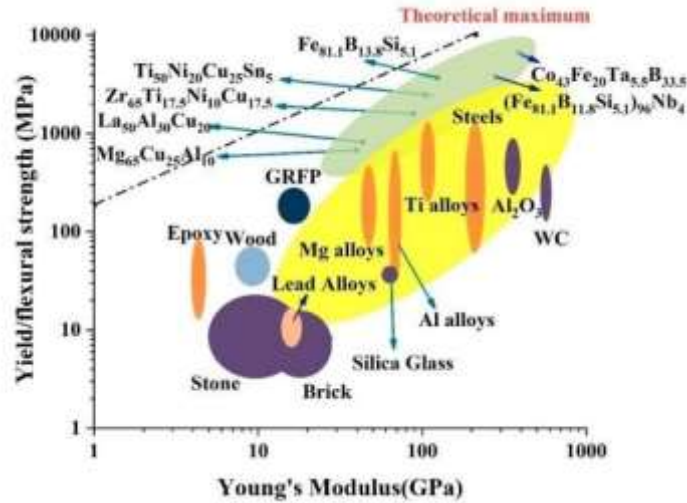


**Fig. 1. 18:** Schematic representation of Yield strength (Polymers, metals, composites, and amorphous alloy) as a function of Young's modulus[35].

The absence of crystalline defects such as dislocation, grain boundaries, and precipitates in amorphous alloys, it exhibits a unique combination of high strength and hardness, high elastic strain, and low Young's modulus in the undercooled liquid zone[15]. Fig.1.19 shows that a comparison of tensile strength, Vicker's hardness and Young's modulus between typical amorphous and conventional crystalline alloys[19]. It can be noted that amorphous alloys possess higher strength and hardness, but relatively lower Young's modulus when compared with traditional crystalline alloys. Among all the BMGs shown in Fig. 1.19, Fe-based BMGs are a special category with a higher strength and hardness value. The elastic modulus is similar to that of traditional stainless steels but the strength and hardness are ~3 to 4 times higher than that of super-high-strength steels[19].

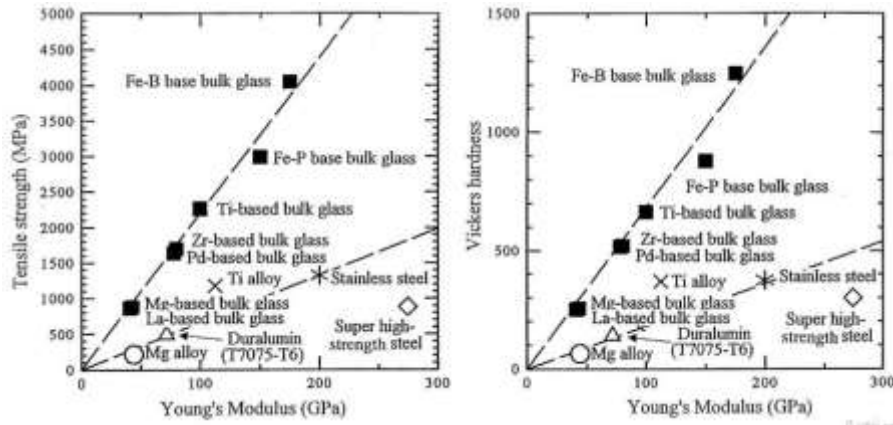


**Fig. 1. 19:** Tensile strength, Vickers hardness versus Young’s modulus for representative alloys in comparison with conventional crystalline alloys[19].

### 1.10 Objectives of the thesis

The interest in research on MGs/BMGs is driven by understanding the structure-property correlation in the absence of long-range order. Such an absence offers a first-rate challenge in predicting their properties. Cooling rate plays a vital role in the formation of MGs/BMGs. There are various methods (based on cooling rate) available in the literature to synthesize BMGs/MGs/glass-nanocomposites. From an alloy design point of view, many criteria for predication of glass formation have been proposed and presented in earlier sections. However, none of these criteria can provide a satisfactory explanation of the GFA of the BMGs. Therefore, the fabrication of Fe-based BMGs is mostly based on the “trial and error” method recently. Synthesis of metallic glass/glass-nanocomposites with better mechanical and other properties is high in demand in the industries. Glass-nanocomposites evolution from metallic glass systems may provide a way to produce advanced material with optimized mechanical properties.

Keeping these in view, four Fe-based metallic glass compositions are selected for studies. Further three different processing routes. These are, (i) Cu-mould casting, (ii) melt-spinning, and (iii) high-energy ball milling. In addition to this, the ball-milled powders were consolidated after 100h of milling through the spark plasma sintering (SPS) technique. The objectives of the present work are focused on:

- (i) The selection of alloy compositions for glass formation based on glass forming criteria given by Azad et al.[34] and further developed as a part of this investigation (cf. chapter 2).

- (ii) The investigation of the effect of three processing routes on the nature of phase evolution and its effect on the indentation behavior.
- (iii) The study about the mode of fracture, shear band formation, and deformation-induced nano-crystallization in metallic glasses.